Intramolecular Electron Transfer in Pentaammineruthenium(III)-Modified Cobaltocytochrome *c*

Ji Sun,[†] Chang Su,[‡] and James F. Wishart*

Department of Chemistry, Brookhaven National Laboratory, Upton, New York 11973

Received June 14, 1996[⊗]

The iron in the heme group of horse-heart cytochrome *c* was replaced by cobalt according to established methods. The resulting cobalticytochrome *c* was subsequently modified at histidine-33 with a pentaammineruthenium group. Proof of correct derivatization was obtained by atomic absorption analysis of cobalt and ruthenium, differential pulse voltammetry, and enzymatic proteolysis analyzed by diode-array HPLC. Cobalt(II)-to-ruthenium(III) intramolecular electron transfer rates were measured as a function of temperature by electron pulse radiolysis. The azide radical ($N_3^{\bullet}$) was used to oxidize the fully reduced form in order to generate the desired electron transfer precursor. The intramolecular electron transfer rate is 1.28 ± 0.04 s^{-1} at 25 °C ($\Delta H^{\ddagger} = 5.7 \pm 0.2$ kcal/mol, $\Delta S^{\ddagger} = -38.7 \pm 0.5$ cal/(deg mol)) for a driving force of 0.28 ± 0.02 eV. The results are compared with those for analogous pentaammineruthenium-modified, native iron, and zinc-substituted cytochromes *c*. The 0.4 eV increase in driving force for intramolecular electron transfer when iron is replaced by cobalt is largely compensated by an increase in reorganization energy.

Introduction

Ruthenium-modified metalloproteins have been employed in electron transfer studies for over 10 years.[1−7] During this time, a wide variety of ruthenium complexes, as well as other types of redox centers, have been attached to cytochromes *c* at various surface residues. Over time, relationships have been found between the intramolecular electron transfer rates and such variables as driving force, reorganization energy, and coupling terms. As a complement to the variety of possible residue modifications, the iron ion from the heme center of native cytochrome *c* can be removed and replaced by a variety of transition-metal ions. This approach has been exploited extensively to study photoinduced electron transfer from porphyrin excited states of Zn-substituted or metal-free cytochrome *c* to pendant redox centers, for example.[6−8] However, these types of substitutions, where electron transfer does not involve the heme metal center and axial ligation is weak or missing, may not retain all of the nuances of the reactivity of this important redox protein.

We chose to investigate electron transfer in cobalt-substituted cytochrome *c* because its properties are much like those of the native form.[9,10] It is six-coordinate and low-spin in both oxidation states. It was expected that electron transfer would be slower due to a larger inner-sphere reorganization contribution. In return, the 400 mV-lower redox potential of the cobalt−heme center would give a higher driving force for intramolecular oxidation than in the iron case. We will show that the previously-reported similarities between cobalt-substituted cytochrome *c* and the native form extend to their intramolecular electron transfer behavior, after reorganization energy and driving force differences are taken into account.

Experimental Section

Materials. Deionized water for all experiments was obtained from a Millipore Milli-Q deionizer. Hexaammineruthenium(III) chloride (Matthey Bishop) was recrystallized from 0.1 M HCl. Sodium formate (Baker Analyzed), sodium phosphate (Baker Analyzed), sodium dithionite (Sigma), sodium azide (Fluka purum), and europium(III) oxide (99.99%, Alfa) were used as supplied. Native horse-heart ferricytochrome *c* (type VI from Sigma) was purified by the method of Brautigan et al.[11] Pentaammineruthenium-modified horse-heart ferricytochrome *c* was prepared by Yocom's procedure.[12]

Preparation of Metal-Free Cyt *c*. Metal-free Cyt *c* was prepared according to refs 6 and 13−15. A 500 mg sample of powdered type VI horse-heart cytochrome *c* was dried by a stream of 40 μm-filtered N_2 gas for 15 min in a Teflon bottle connected to an all-Teflon gas manifold. The sample was cooled by application of a liquid-N_2-filled Dewar flask to the bottle. HF (Matheson) was introduced into

[†] Present address: IGEN, Inc., 16020 Industrial Dr., Gaithersburg, MD 20877.

[‡] Present address: Department of Molecular Sciences, Hoffmann-La Roche Co., 340 Kingsland Ave., Nutley, NJ 07110-1199.

[⊗] Abstract published in *Advance ACS Abstracts,* September 1, 1996.

(1) Winkler, J. R.; Nocera, D. G.; Yocom, K. M.; Bordignon, E.; Gray, H. B. *J. Am. Chem. Soc.* **1982**, *104*, 5798−5800.
(2) Isied, S. S.; Worosila, G.; Atherton, S. J. *J. Am. Chem. Soc.* **1982**, *104*, 7659−7661.
(3) Isied, S. S.; Kuehn, C.; Worosila, G. *J. Am. Chem. Soc.* **1984**, *106*, 1722−1726.
(4) Nocera, D. G.; Winkler, J. R.; Yocom, K. M.; Bordignon, E.; Gray, H. B. *J. Am. Chem. Soc.* **1984**, *106*, 5145−5150.
(5) Bechtold, R.; Gardineer, M. B.; Kazmi, A.; van Hemelryck, B.; Isied, S. S. *J. Phys. Chem.* **1986**, *90*, 3800−3804.
(6) (a) Elias, H.; Chou, M. H.; Winkler, J. R. *J. Am. Chem. Soc.* **1988**, *110*, 429-434. (b) Meade, T. J.; Gray, H. B.; Winkler, J. R. *J. Am. Chem. Soc.* **1989**, *111*, 4353−4356. (c) Therien, M. J.; Selman, M.; Gray, H. B.; Chang, I-J.; Winkler, J. R. *J. Am. Chem. Soc.* **1990**, *112*, 2420−2422.
(7) Winkler, J. R.; Gray, H. B. *Chem. Rev.* **1992**, *92*, 369−379.
(8) Magner, E.; McLendon, G. *J. Phys. Chem.* **1989**, *93*, 7130−7134.
(9) Dickinson, L. C.; Chien, J. C. W. *Biochemistry* **1975**, *14*, 3534−3542.
(10) (a) Moore, G. R.; Williams, R. J. P.; Chien, J. C. W.; Dickson, L. C. *J. Inorg. Biochem.* **1980**, *12*, 1−15. Note that the final author's name should have been spelled Dickinson. (b) Boswell, A. P.; Moore, G. R.; Williams, R. J. P.; Chien, J. C. W.; Dickinson, L. C. *J. Inorg. Biochem.* **1980**, *13*, 347−352.
(11) Brautigan, D. L.; Ferguson-Miller, S.; Margoliash, E. *Methods Enzymol.* **1978**, *53*, 128−164.
(12) Yocom, K. M.; Shelton, J. B.; Shelton, J. R.; Schroeder, W. A.; Worosila, G.; Isied, S. S.; Bordignon, E.; Gray, H. B. *Proc. Natl. Acad. Sci. U.S.A.* **1982**, *79*, 7052−7055.
(13) Flatmark, T.; Robinson, A. B. Structure and Function of Cytochrome; Okunuki, K., Kamen, M. D., Sekuzu, I., Eds.; University Park Press: Baltimore, MD, 1986; pp 383−387.
(14) Fisher, W. R.; Taniuchi, H.; Anfinsen, C. B. *J. Biol. Chem.* **1973** , *248*, 3188−3195.
(15) Vanderkooi, J. M., Adar, F.; Erecinska, M. *Eur. J. Biochem.* **1976**, *64*, 381−387.

S0020-1669(96)00715-X CCC: $12.00 © 1996 American Chemical Society

the N_2 gas stream until approximately 5 mL of liquid HF had condensed onto the sample. The color of the cytochrome *c* immediately changed from red to purple. After 2−3 min, the sample was allowed to warm to room temperature. HF was removed by a constant flow of N_2 over the course of 1 h. (*Safety note*: The HF thus evaporated from the reaction vessel was trapped by bubbling through a 1 M KOH/8 M K_2CO_3 solution in a Teflon bottle.) The resultant residue was gradually dissolved in 80 mL of 50 mM ammonium acetate at pH 5. The solution was repeatedly washed with 85 mM phosphate buffer at pH 7 in an Amicon ultrafiltration unit with a YM3 membrane. The sample was applied to a Whatman CM-52 column (2.5 in. × 18 in.) and eluted with 100 mM phosphate buffer (pH 7.0). The major band was collected. A minor band preceded the major band, and some denatured protein stuck to the top of the column. The yield was about 45% by absorbance. Metal-free cytochrome *c* was protected from light as much as possible during all steps. All glassware used in the handling of metal-free cytochrome *c* was rinsed with concentrated acetic acid, followed by deionized water, to avoid contamination from trace metals such as copper.

Preparation of Cobalticytochrome *c*. Cobalt-substituted cytochrome *c* was prepared according to the method of Dickinson and Chien.[16] Metal-free cytochrome *c* (200 mg, or 0.25 mM) was added to a septum-capped flask containing a pH 5 solution of 50 mM ammonium acetate under a stream of Ar or N_2, heated by a 65 °C water bath. A 15-fold excess of $Co(OAc)_2$ was added and the mixture allowed to react for 15−20 min. The solution was cooled to room temperature and exposed to air. The crude cobalt-substituted cytochrome *c* was then repeatedly washed with phosphate buffer at pH 7 in an Amicon concentrator. The sample was purified on a CM-52 column by elution with 200 mM pH 7 phosphate buffer. There was only one major band. Some denatured protein was found on the top of the column. The sample was again concentrated by ultrafiltration and further purified on a second CM-52 column eluted with 85 mM pH 7 phosphate buffer. The major band was collected. The yield was approximately 33%.

Preparation of Pentaammineruthenium(III)−Cobalticytochrome *c*. The pentaammineruthenium derivative of CoCyt *c* was prepared according to the literature method for modifying the native protein.[12] CoCyt *c* was reacted with a 15-fold excess of $[Ru(NH_3)_5H_2O]^{2+}$ in 100 mM pH 7 HEPES buffer under argon at room temperature for 17−18 h. The CoCyt *c* concentration was about 0.75 mM. The mixture was then repeatedly washed with 100 mM pH 7 HEPES buffer and then 50 mM pH 7 HEPES, in an Amicon ultrafiltration unit (MWCO 3000), and applied to a CM-52 column. A band eluted consisting of a small amount of unmodified CoCyt *c*, followed by a Ru-containing band. The second band was identified as $(NH_3)_5Ru(His_{33})$−Cyt *c* by HPLC analysis of endoproteinase digestion products (see Results and Discussion). Atomic absorption analysis of the purified His_{33}-ruthenated cobalticytochrome showed ratios of ruthenium to cobalt of 0.92:1 and 1.09:1 for two typical preparations.

Enzymatic Proteolysis and HPLC. Tryptic digestions of Ru-modified and unmodified Co^{III}Cyt *c* and native and Ru-modified iron Cyt *c* were performed according to ref 12. In another series of experiments, modified and unmodified Fe and Co cytochromes (0.1−0.5 mg) were reacted with 5 μg of *Lysobacter enzymogenes* endoproteinase Lys-C (Calbiochem) at 37 °C for 5 h in 500 mM Tris buffer at pH 8.5 according to the method of Jekel et al.[17] HPLC chromatographic analyses of the protein digests were conducted using a Waters HPLC system including a Model 990 diode-array detector. A Vydac C18 reverse-phase polypeptide column (Catalog No. 218TP54) was used, and the column was eluted with a gradient starting at 0.1% (v/v) trifluoroacetic acid in water and ending at 60% acetonitrile in 120 min.

Electrochemistry. Differential pulse voltammetry of a solution of 100 μM pentaammineruthenium-modified cobalticytochrome c in 50 mM pH 7.0 phosphate buffer was conducted at a bis(4-pyridyl) disulfide-modified[18] gold disk electrode with a Bioanalytical Systems Model 100A electrochemical analyzer. The reference electrode was saturated sodium calomel (+236 mV vs NHE).

UV−Vis and Circular Dichroism Spectra. UV−vis spectra of the cytochrome solutions in 50 mM pH 7 phosphate buffer were recorded on a Hewlett-Packard 8452A diode-array spectrophotometer. Circular dichroism spectra were measured in 50 mM pH 7 phosphate buffer with a Jasco J-500 spectropolarimeter controlled by an IBM PC through a Jasco IF-500 serial interface. A cylindrical CD cell with a 1 cm path length was used.

Pulse Radiolysis. Electron pulse-radiolysis transient-absorption experiments were carried out with the 2 MeV Van de Graaff accelerator at Brookhaven National Laboratory using a PC-controlled, CAMAC-based data acquisition and control system. The experiments were done using an all-quartz pulse radiolysis cell consisting of a 50 mL reservoir with an outlet which drains into a 20 mm long, 10 mm high, 5 mm deep rectangular optical cell where the sample is irradiated (through the short dimension) and probed by light through the long dimension (2.0 and 6.1 cm path lengths). Irradiated solutions are drained from the cell after use, so the solution in the reservoir remains fresh until it is used. The carbon dioxide radical anion, $CO_2^{\bullet-}$, was produced by the reaction of the radiolytically-generated hydroxyl radical ($^\bullet$OH) with the formate ion (0.1 M HCOONa) in N_2O-saturated water (reactions 1−3). The azide radical, $N_3^\bullet$, was produced by the reaction of $^\bullet$OH with the azide ion (1 mM NaN_3) in N_2O-saturated water (reactions 1, 2, and 4). Radiolytic dose levels were chosen such that the concentrations of oxidizing or reducing radicals produced in a single shot were no more than 15% of the cytochrome concentration. Radiolysis pulse widths were between 60 and 120 ns. The buffer was 50 mM sodium phosphate, pH 7.0, in all cases.

$$H_2O \xrightarrow{2\ \text{MeV electrons}} e_{aq}^-,\ ^\bullet OH,\ H^\bullet,\ H_2,\ H_2O_2 \quad (1)$$

$$e_{aq}^- + N_2O + H_2O \rightarrow N_2 + {}^\bullet OH + OH^- \quad (2)$$

$$^\bullet OH + HCO_2^- \rightarrow H_2O + CO_2^{\bullet-} \quad (3)$$

$$^\bullet OH + N_3^- \rightarrow OH^- + N_3^\bullet \quad (4)$$

Reductive preparations of cobaltocytochrome *c* and ruthenium-modified cobaltocytochrome *c* for pulse radiolysis experiments were performed in an argon-filled glovebox (Vacuum Atmospheres). The modified or unmodified cobalticytochrome *c* was reduced with an large excess of sodium dithionite (50 mM), which was then removed by repeated ultrafiltration over a 3000 Da molecular mass cutoff membrane using argon-saturated 50 mM phosphate buffer. Meanwhile, 15−50 mL of phosphate buffer solution containing 1 mM sodium azide was saturated with N_2O in a pulse radiolysis reservoir cell. The reduced cobaltocytochrome *c* solution was diluted to the desired concentration and placed in a syringe for transfer out of the glovebox. The solution was introduced into the pulse radiolysis cell through a rubber septum via an 18-gauge platinum needle. The final concentration of cobaltocytochrome *c* in the pulse radiolysis solution (normally 2−20 μM) was determined by using a Hewlett-Packard 8452A diode-array spectrophotometer to measure the absorbance of samples drained from the radiolysis cell (after the first two samples were discarded) as fully oxidized protein after exposure to air (ϵ_{426} = 106 100 M^{-1} cm^{-1}, ϵ_{567} = 7770 M^{-1} cm^{-1}).[19]

In some instances it was observed that the reduced CoCyt *c* had become oxidized through exposure to inadvertent oxidants during handling. In those cases, the protein was reduced in situ by the addition of 1−2 equiv of europous perchlorate/equiv of CoCyt *c* to the reservoir of the pulse radiolysis cell. (The europous perchlorate solution was prepared by dissolution of Eu_2O_3 in dilute $HClO_4$, followed by reduction over Zn/Hg.) At the concentrations used here, excess Eu^{2+} may intercept the azide radical, thereby reducing the yield of oxidized ruthenium and cobalt sites, and it can also re-reduce the ruthenium center, which results in an observed rate at 434 nm which is faster

(16) Dickinson, L. C.; Chien, J. C. W. *Biochemistry*, **1975**, *14*, 3526−3534.
(17) Jekel, P. A.; Weijer, W. J.; Beintema, J. J. *Anal. Biochem.* **1983**, *134*, 347−354.
(18) Taniguchi, I.; Toyosama, K.; Yamaguchi, K. *J. Electroanal. Chem.* **1982**, *140*, 187.
(19) Chien, J. C. W. *J. Phys. Chem.* **1978**, *82*, 2171−2179.

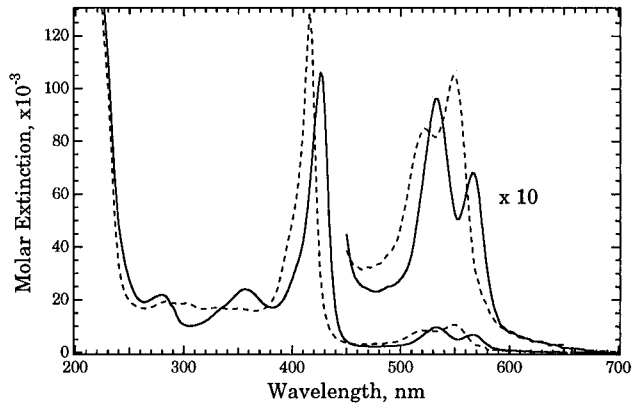

Figure 1. UV−vis absorption spectra of cobaltocytochrome *c* (dotted line) and cobalticytochrome *c* (solid line) in 50 mM pH 7 phosphate buffer. The spectra are normalized to the extinction coefficients reported by Dickinson and Chien[16] (Co^{II}, $\epsilon_{416.5} = 128\,700\ M^{-1}\ cm^{-1}$; Co^{III}, $\epsilon_{426} = 106\,100\ M^{-1}\ cm^{-1}$).

than the true Co-to-Ru intramolecular electron transfer rate. Fifteen minutes after addition, the excess Eu^{2+} in a given 2 mL fill of the irradiated part of the cell was oxidatively titrated by the application of successive radiolytic doses until the change in absorbance at 434 nm had grown to the proper magnitude and the observed first-order rate had decreased to a constant value over several shots. Over time, the excess Eu^{2+} in the reservoir was consumed, so successive fills required less titration and eventually none at all.

Stopped-Flow Measurements. Stopped-flow kinetic measurements were carried out using a DX.17MV/S stopped-flow spectrofluorimeter (Applied Photophysics, Leatherhead, U.K.). Observed first-order rates were fit to the data using the software supplied with the instrument. The anaerobic protocol specified by the manufacturer was followed. The protocol requires that the complete flow circuit should first be flushed with deoxygenated 50 mM pH 8 Tris/HCl buffer, filled for 12 h with a 5 mM solution of sodium dithionite in the same buffer, and flushed thoroughly with deoxygenated buffer before use. The closed-circuit thermostating bath was also treated with sodium dithionite in Tris buffer and purged continuously with nitrogen gas before and during experiments. For the measurement of rates of intermolecular oxidation of cobaltocytochrome *c* by hexaammineruthenium(III) ion or ferricytochrome *c*, the oxidant was used in excess to ensure pseudo-first-order kinetics and insensitivity of the observed rate to prior, inadvertent oxidation of the cobaltocytochrome *c*. All experiments were performed in 50 mM pH 7 phosphate buffer (μ = 0.1 M). For determination of the second-order rate constant, the concentration of hexaammineruthenium(III) chloride was varied from 1 to 10 mM while the cobaltocytochrome concentration was fixed at 20.3 μM. Intermolecular electron transfer rates were measured over a range of temperatures from 6 to 45 °C. The concentrations of $[Ru(NH_3)_6]^{3+}$ and cobaltocytochrome *c* for the activation parameter determination were 10.0 mM and 24.6 μM, respectively.

Results and Discussion

Preparation and Characterization. The earlier work of Dickinson and Chien[9,16,19] established the fact that the two-step procedure to replace the iron ion in horse-heart cytochrome *c* with cobalt results in a high yield of reconstituted protein which shows strong structural similarity to the native protein. They demonstrated that the inserted cobalt ion remains six-coordinate in both oxidation states. Modification of the cobalt-substituted horse-heart cytochrome *c* with $[Ru(NH_3)_5H_2O]^{2+}$ occurs with the same efficacy as the modification of the native, iron-containing cytochrome *c*.[4,12] The ruthenated fraction is modified at His_{33}, as in the iron case. In two preparations, the major ruthenated band showed ruthenium-to-cobalt ratios of 0.92:1 and 1.09:1 by atomic absorption analysis.

Absorption Spectroscopy. UV−vis spectra of Co^{II}Cyt *c* and Co^{III}Cyt *c* are shown in Figure 1. Addition of the pentaammineruthenium group does not affect the absorbance spectra to any measurable extent in either oxidation state. The spectra agree with those previously reported by Chien.[16] Although the wavelengths of the Soret-, α-, and β-band maxima are the same for Fe^{II}Cyt *c* and Co^{II}Cyt *c*, the 550 nm α band which is so prominent in the native iron spectrum is only about half as strong for the cobalt-substituted cytochrome. When the cobalt cytochrome is oxidized, the most significant change in the spectrum is the large shift in the Soret-band maximum from 416.5 to 426 nm. Smaller changes occur in the α- and β-band regions. The large extinction coefficient change at 434 nm, due to the Soret shift, and the relatively low background absorbance there make it the most favorable place to observe the electron transfer kinetics.

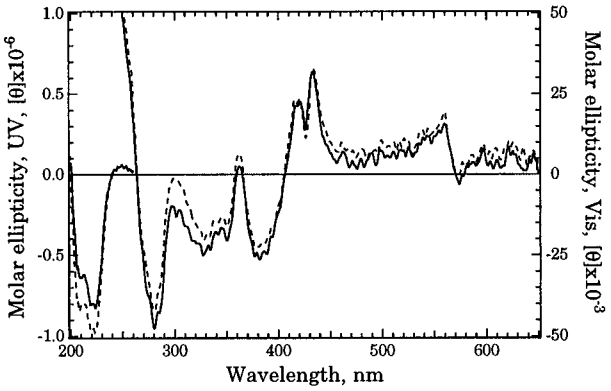

Figure 2. Circular dichroism spectra of cobalticytochrome *c* (dashed line) and pentaammineruthenium-modified cobalticytochrome *c* (solid line) in 50 mM pH 7 phosphate buffer.

Circular Dichroism. Circular dichroism spectra of cobalticytochrome *c* and pentaammineruthenium-modified cobalticytochrome *c* were each recorded at concentrations of 2.1 μM for the UV spectrum and 10.5 μM for the visible spectrum in 50 mM pH 7 phosphate buffer. (See Figure 2. The CD spectrum of cobaltocytochrome *c* under the same conditions is presented in the Supporting Information.) Throughout the visible spectrum, the modification of cobalticytochrome *c* by the ruthenium group has very little effect on the spectral features, which primarily originate from the heme chromophore.[20] In the ultraviolet region, the negative peaks at 209 and 222 nm, which are associated with the presence of helical regions, are slightly reduced in intensity after ruthenium modification. Chien has previously reported[21] the helicity of cobalticytochrome *c* as 22.2% based on the formula $[\theta']_{222} = -30300f_H - 2340$,[22,23] where the mean residue ellipticity $[\theta']_{222} = [\theta]_{222}/104$ residues and f_H is the fraction of helical content. Our measurements of molar ellipticities at 222 nm for Co^{III}Cyt *c* (-9.76×10^5 deg cm^2/dmol), $(NH_3)_5Ru-Co^{III}$Cyt *c* (-8.25×10^5 deg cm^2/dmol), and Co^{II}Cyt *c* (-1.06×10^6 deg cm^2/dmol) result in calculated helicities of 23.2, 18.5, and 26.0%, respectively.

In their review of CD studies of heme proteins,[20] Myer and Pande pointed out the variance of helicities calculated for heme proteins by different methods, as well as the problem of spectral interference from the heme prosthetic group, particularly in proteins with low helical content, such as cytochrome *c*. We find, however, that the cobalticytochrome *c* prepared in our laboratory has the same helicity as that prepared by Chien and co-workers and that ruthenium modification reduces the helicity

(20) Myer, Y. P.; Pande, A. In The Porphyrins; Dolphin, D., Ed.; Academic Press: Ed.; New York, 1978; Vol. 3, pp 271−322.
(21) Chien, J. C. W. *J. Phys. Chem.* **1978**, *82*, 2158−2171.
(22) Snyder, F. W., Jr.; Chien, J. C. W. *J. Mol. Biol.* **1979**, *135*, 315−325.
(23) Chen, Y. H.;Yang, J. T.; Martinez, H. M. *Biochemistry* **1972**, *11*, 4120−4131.

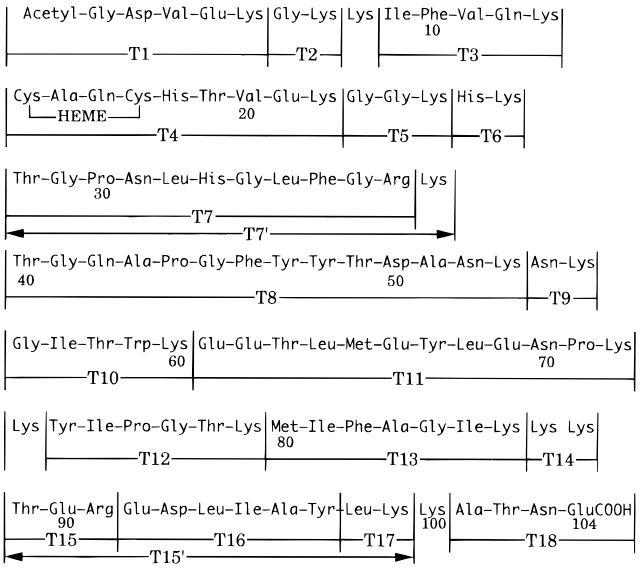

Figure 3. Tryptic digestion map of horse-heart cytochrome *c*, from ref 12. Locations where the endoproteinase Lys-C digestion map is expected to differ are indicated.

Scheme 1

$$\begin{array}{ccccc} \mathrm{Fe^{III}}\text{-Cyt } c & \Rightarrow & \mathrm{Fe^{III}}\text{-Cyt } c & \Rightarrow & \mathrm{Co^{III}}\text{-Cyt } c \\ \text{(Trypsin)} & & \text{(Endo)} & & \text{(Endo)} \\ & & \Downarrow & & \Downarrow \\ (\mathrm{NH_3})_5\mathrm{Ru}\text{-}\mathrm{Fe^{III}}\text{-Cyt } c & \Rightarrow & (\mathrm{NH_3})_5\mathrm{Ru}\text{-}\mathrm{Fe^{III}}\text{-Cyt } c & \Rightarrow & (\mathrm{NH_3})_5\mathrm{Ru}\text{-}\mathrm{Co^{III}}\text{-Cyt } c \\ \text{(Trypsin)} & & \text{(Endo)} & & \text{(Endo)} \end{array}$$

by a small amount. No decrease in helicity had been observed in $(NH_3)_5Ru-Fe^{III}$Cyt *c* compared to ferricytochrome *c*.[3] According to the published X-ray crystal structure of horse-heart ferricytochrome *c*,[24] the only helical region in the protein which is near the His_{33} modification site is the one near the C-terminus of the peptide sequence (residues 87−102). None of the residues in the region between His_{33} and the heme group are in helical sequences.

Electrochemistry. Dickinson and Chien[16] measured the reduction potential of cobalt-substituted cytochrome *c* as −0.14 ± 0.02 V vs NHE by potentiometric titration. Our differential pulse voltammetry results, obtained at a bis(4-pyridyl) disulfide-modified gold disk electrode, show a peak potential of −0.17 V vs NHE. Inspection of the cobalt DPV peak (Supporting Information) reveals that it is asymmetrically broadened by a slow heterogeneous electron transfer rate, in keeping with the very low self-exchange rate constant for CoCyt *c* estimated by Chien[21,25] and the observations reported here. The effect of the slow heterogeneous electron transfer rate is to displace the apparent peak potential in a cathodic scan to a more negative value with respect to the fast, reversible case. A theoretical treatment of the effects of quasi-reversible and irreversible behavior on polarograms was recently published by Kim et al.[26] Work on quantification of the quasi-reversibility of the CoCyt *c* couple is continuing. Our measurements are consistent with Chien's result; we will use the potentiometric titration value of −0.14 ± 0.02 V vs NHE in subsequent calculations. The DPV wave from the ruthenium couple has a normal width, and the formal potential is the same (+0.14 V vs NHE) as in the corresponding pentaammineruthenium-modified iron cytochrome *c*.

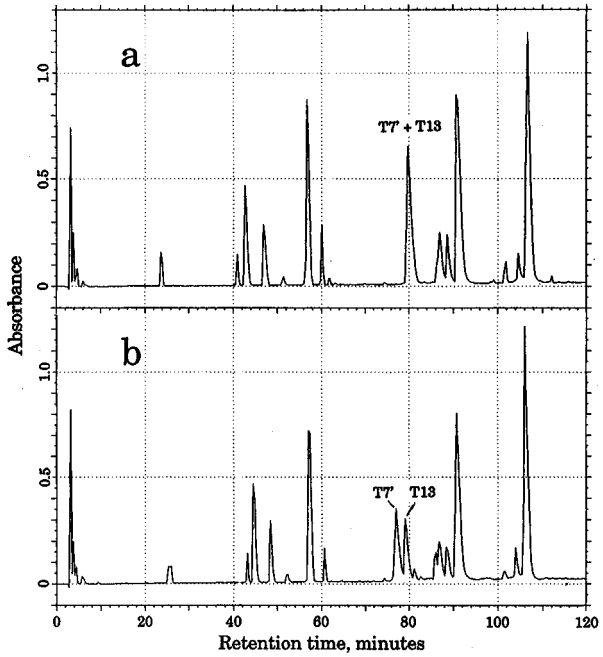

Figure 4. Elution profiles at 220 nm of the endoproteinase Lys-C digestion products of ferricytochrome *c* (a) and pentaammineruthenium-modified ferricytochrome *c* (b).

Enzymatic Proteolysis. It was found that Co^{III}Cyt *c* is very resistant to tryptic digestion, a situation which might be anticipated from the well-known substitution inertia of Co^{III}. Moore et al.[10] have also noted that the axial Met80 ligand of cobalticytochrome *c* is not displaced by OH^- even at pH 11, whereas it is displaced at pH 9.2 in ferricytochrome *c*. The efficiency of tryptic digestion of CoCyt *c* was *not* improved by the addition of excess sodium dithionite or sodium ascorbate to keep the cobalt in the reduced state. In all cases, the HPLC chromatograms displayed large numbers of small peaks which did not bear much relation to the known digestion pattern of ferricytochrome *c*, followed by massive peaks at very long retention times indicative of mostly intact protein.

In contrast, Co^{III}Cyt *c* is effectively digested by *Lysobacter enzymogenes* endoproteinase Lys-C. The reaction was performed according to the method of Jekel et al.[17] Modified and unmodified Fe and Co cytochromes *c* (0.1−0.5 mg) were reacted with 5 μg of endoproteinase Lys-C (Calbiochem) at 37 °C for 5 h in 0.5 M Tris buffer at pH 8.5. The chromatogram resulting from endoproteinase Lys-C digestion of native iron horse-heart Cyt *c* is similar to that obtained from tryptic digestion, since both enzymes cleave peptides on the carboxylate side of lysine residues. Trypsin also cleaves at arginine residues, of which horse-heart cytochrome has only two. Consequently, the major bands of the endoproteinase Lys-C digestion chromatograms may be assigned by analogy to previously identified tryptic digestion fractions, if eluted under the same conditions. The tryptic digestion map of horse-heart cytochrome *c* deduced by Yocom et al.[12] is shown in Figure 3. Locations where the endoproteinase Lys-C digestion map is expected to differ are also indicated in the map. In this way, chromatographic band assignments were made by analogy according to Scheme 1.

HPLC chromatograms of endoproteinase-digested native and ruthenium-modified horse-heart ferricytochrome *c*, recorded at 220 nm, are shown in Figure 4, while the corresponding chromatograms for cobalt-substituted cytochrome *c* are shown in Figure 5. Chromatograms for the same runs, recorded at 300 and 420 nm, are provided as Supporting Information. The

(24) Bushnell, G. W.; Louie, G. V.; Brayer, G. D. *J. Mol. Biol.* **1990**, *214*, 585−595.
(25) Chien, J. C. W.; Gibson, H. L.; Dickinson, L. C. *Biochemistry* **1978**, *17*, 2579−2584.
(26) Kim, M.-H.; Smith, V. P.; Hong, T.-K. *J. Electrochem. Soc.* **1993**, *140*, 712−721.

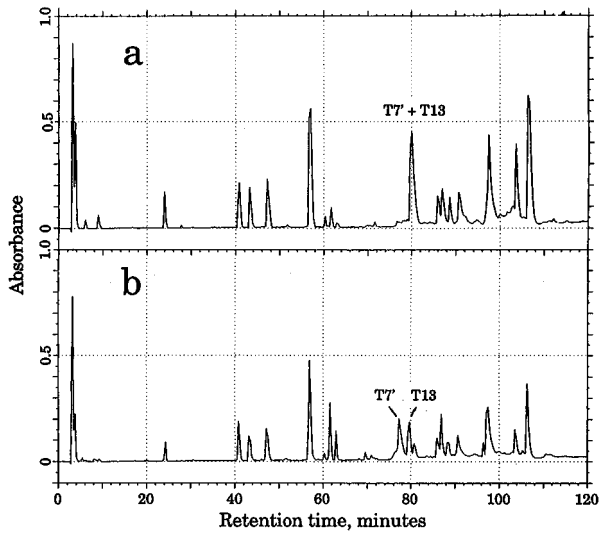

Figure 5. Elution profiles at 220 nm of the endoproteinase Lys-C digestion products of cobalticytochrome *c* (a) and pentaammineruthenium-modified cobalticytochrome *c* (b).

Table 1. Reverse-Phase HPLC Retention Times (min) for Selected Peptide Fragments from Trypsin and Endoproteinase Lys-C Digestion of Horse-Heart Ferri- and Cobalticytochrome *c* and Pentaammineruthenium-Modified Ferri- and Cobalticytochrome *c*[a]

Trypsin

peptide	T10	T13	T7	shift[b]	T4
native Fe hh Cyt *c*	61.0	81.6	84.8		90.4
$(NH_3)_5Ru(His_{33})-$FeCyt *c*	61.0	81.2	82.2	−2.6	90.4

Endoproteinase Lys-C

peptide	T10	T13	T7′	shift[b]	T4
native Fe hh Cyt *c*	61.0	[80.5	80.5][c]		91.4
$(NH_3)_5Ru(His_{33})-$FeCyt *c*	61.0	79.9	77.7	−2.8	91.2
Co(III) hh Cyt *c*	62.6[d]	[80.8	80.8][c]		91.6
$(NH_3)_5Ru(His33)-$CoCyt *c*	62.5[d]	80.4	78.3	−2.5	91.4

[a] Conditions: Vydac C18 column; 0.1% (v/v) trifluoroacetic acid; A: water; B, acetonitrile; 0−60% B in 120 min, 0.8 mL/min. [b] Shift of T7 or T7' band due to attachment of $(NH_3)_5Ru^{III}$. [c] Co-elution. [d] Largest of three closely-spaced peaks.

chromatograms for ferricytochrome in Figure 4 contain fewer bands than those of corresponding tryptic digests (see Figures 2 and 3 of ref 9). Identification of all the peaks in the chromatogram is beyond the scope of this report; however, two peaks are particularly easy to identify due to characteristic absorption bands at longer wavelengths. Fragment T10 contains tryptophan-59 (detectable at 300 nm) and elutes around 61 min under our conditions, while the heme-containing fragment T4 elutes around 91 min (detectable at 420 nm). Both of these bands elute at the same times regardless of whether trypsin or endoproteinase is used for digestion (see Table 1).[27]

Beyond the analogy between tryptic and endoproteinase cleavage patterns, further proof of the correct identification of the band containing the His_{33} modification target site makes use of the above-mentioned difference in cutting loci between the two enzymes. The 11-peptide tryptic digestion fragment which includes His_{33}, identified in ref 6 as T7, is terminated at arginine (Arg_{38}). When endoproteinase Lys-C cleaves the protein, this fragment is lengthened by one lysine (the longer fragment is referred to henceforth as T7′). The additional positive charge due to the lysine residue causes the T7′ band to elute from the C-18 column approximately 4 min earlier than T7 under the same conditions, adding support to its identification. When T7′ is unmodified, it co-elutes with T13 at about 80.7 min, as indicated by brackets in Table 1.

The HPLC chromatograph of the endoproteinase digestion products of cobalticytochrome *c* in Figure 5a exhibits some differences with the ferricytochrome *c* chromatograph in Figure 4a, particularly in the marker bands T10 and T4. T10 has been split into three peaks, still grouped between 60 and 64 min. The T4 band has been split into three major fragments, the first of which elutes at the characteristic time of 91 min, followed by others at 97.5 and 103 min. In addition, the elution profile at 420 nm indicates a background of minor, heme-containing bands beginning at 76 min and continuing to the end of the chromatogram. From differences described here, it is clear that cobalticytochrome *c* is also somewhat resistant to endoproteinase digestion in comparison to ferricytochrome *c*, fortunately this resistance is not enough to prevent characterization. It is even more fortunate that the T7′ and T13 bands behave in exactly the same fashion regardless of whether the protein contains iron or cobalt.

HPLC analysis of the endoproteinase digestion products of the second, ruthenated band of cobalticytochrome *c* from the CM-52 column indicates that the protein is modified on the T7' fragment, presumably at His_{33}. Addition of the $[(NH_3)_5Ru]^{3+}$ group to the T7 and T7′ fragments causes them to elute about 2.6 min earlier under our HPLC conditions (see Table 1). The same shift is observed for trypsin and endoproteinase Lys-C and for iron- and cobalt-containing proteins. The fragments identified as ruthenated T7′ from the endoproteinase digestion of the cobalt and iron proteins have characteristic spectra for the $[(NH_3)_5Ru^{III}(\text{histidine})]^{3+}$ chromophore (see Figure 6). Ruthenium-modified T7′ is clearly resolved from T13, which elutes 2 min later.

Electron Transfer Reactions. (a) Reduction of Cobalticytochrome *c* by the Carbon Dioxide Radical Anion. The rate of reduction of Co^{III}Cyt *c* by $CO_2^{\bullet-}$ was measured at cobalticytochrome *c* concentrations of 2.0 and 11.6 μM. The N_2O-saturated solution contained 50 mM pH 7 sodium phosphate buffer and 0.1 M sodium formate. The observed rates at the two concentrations were 300 ± 60 and 1600 ± 200 s^{-1}, respectively, which gives a rate constant of 1.4×10^8 M^{-1} s^{-1} for the reaction

$$CO_2^{\bullet-} + Co^{III}\text{Cyt } c \rightarrow CO_2 + Co^{II}\text{Cyt } c \qquad (5)$$

The corresponding rate constant[3] for native ferricytochrome is 1.8×10^9 M^{-1} s^{-1}.

(b) Oxidation of Cobaltocytochrome *c* by the Azide Radical. Due to the sensitivity of cobaltocytochrome *c* toward oxidation, the concentration of the reduced form in a given experiment is prone to some uncertainty. It is possible to calculate a reasonably close lower limit to the second-order rate constant despite the uncertainty. For example, first pulses on three fresh samples of 6.9 μM cobaltocytochrome *c* in N_2O-saturated, 50 mM pH 7.0 sodium phosphate buffer containing 1.0 mM sodium azide gave observed first-order rates of 5730, 5260, and 5550 s^{-1} for the process

$$N_3^{\bullet} + Co^{II}\text{Cyt } c \rightarrow N_3^- + Co^{III}\text{Cyt } c \qquad (6)$$

The rate constant estimated from these results is (8.0 ± 0.3) ×

(27) For endoproteinase digestions of ferricytochrome, the T10 band is significantly reduced in intensity with respect to T4 as compared to tryptic digestions. It seems likely that the yield of T10 is reduced by inefficient cleavage and that most of the tryptophan-59 residue is contained in a much longer peptide eluting at 106.5 min which also appears in the 300 nm elution profile.

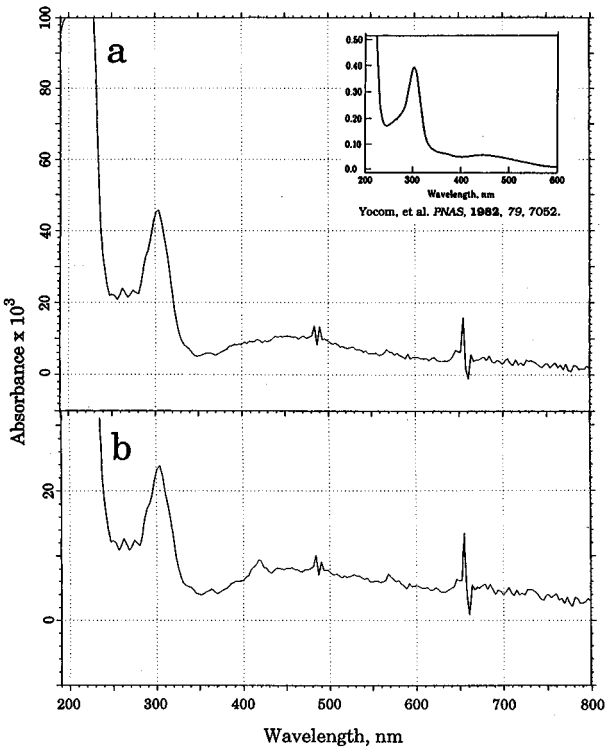

Figure 6. Diode-array HPLC spectra of the ruthenium-modified T7′ peptide fragments from endoproteinase Lys-C digestion products of pentaammineruthenium-modified ferricytochrome *c* (a; inset is the spectrum of $[(NH_3)_5Ru^{III}(histidine)]^{3+}$ from ref 12) and pentaammineruthenium-modified cobalticytochrome *c* (b; noise due to lower concentration).

10^8 M^{-1} s^{-1}, not much smaller than the 1.3×10^9 M^{-1} s^{-1} reported for ferrocytochrome.[28]

(c) Oxidation of Cobaltocytochrome *c* by Hexaammineruthenium(III). Stopped-flow kinetics were used to determine the rate of oxidation of Co^{II}Cyt *c* by $[Ru^{III}(NH_3)_6]^{3+}$:

$$[Ru^{III}(NH_3)_6]^{3+} + Co^{II}\text{Cyt } c \rightarrow [Ru^{II}(NH_3)_6]^{2+} + Co^{III}\text{Cyt } c \quad (7)$$

In order to minimize the effect of inadvertent oxidation, pseudo-first-order conditions were used with $[Ru^{III}(NH_3)_6]^{3+}$ in large excess. The concentration of the ruthenium complex was varied by a factor of 10. When the observed rates are plotted as a function of concentration (see the Supporting Information), the second-order rate constant is 10.3 ± 0.1 M^{-1} s^{-1} (intercept = 2×10^{-3} s^{-1}). An Eyring plot of the temperature dependence of the second-order rate (see Figure 8) yields $\Delta H^{\ddagger} = 8.38 \pm 0.06$ kcal/mol, $\Delta S^{\ddagger} = -26.0 \pm 0.2$ cal/(deg mol).

In the case of FeCyt *c*, the driving force pushes the analog of reaction 7 to the left by about the same amount that drives reaction 7 forward in the cobalt case: the reduction potential of $[Ru^{III}(NH_3)_6]^{3+}$ is *lower* than that of FeCyt *c* by 0.2 eV. In the native iron case, the intermolecular electron transfer rate constant for heme reduction[4] is 6.7×10^4 M^{-1} s^{-1}. The fact that the intermolecular electron transfer rate for the cobalt case is 6700 times slower for approximately the same driving force means that the self-exchange rate constant for Co^{II}Cyt *c* is very low.

(d) The Electron Transfer Self-Exchange Rate Constant of CoCyt *c*. Chien and co-workers[19,25] attempted to directly determine the self-exchange rate of CoCyt *c* by measuring the ^{1}H NMR spin−lattice relaxation time of the ring-current-shifted Met_{80} methyl resonance of diamagnetic Co^{III}Cyt *c* in the presence of paramagnetic Co^{II}Cyt *c*. They could not observe any evidence for exchange and therefore set an upper limit of 133 M^{-1} s^{-1} for the process.

In the same report,[25] however, they were able to estimate the self-exchange rate by application of theoretical cross-relations to the oxidation of cobaltocytochrome *c* by ferricytochrome *c*.

$$Co^{II}\text{Cyt } c + Fe^{III}\text{Cyt } c \rightarrow Co^{III}\text{Cyt } c + Fe^{II}\text{Cyt } c \quad (8)$$

They obtained a second-order rate constant of 8300 M^{-1} s^{-1} (μ = 0.1 M, pH 7, 25 °C) for reaction 8, from which they calculated a $Co^{II/III}$Cyt *c* self-exchange rate constant of 5.1×10^{-3} M^{-1} s^{-1} from nonadiabatic electron-tunneling theory,[29] using a self-exchange rate of 8100 M^{-1} s^{-1} for ferricytochrome *c*. They also applied the Marcus cross-relation[30,31]

$$k_{12} = (k_{11} k_{22} K_{12} f_{12})^{1/2} W_{12} \quad (9)$$

$$W_{12} = \exp[-(w_{12} + w_{21} - w_{11} - w_{22})/2RT] \quad (10)$$

$$\ln f_{12} = (\ln K_{12})^2/4 \ln(k_{11}k_{22}/Z^2) \quad (11)$$

to their results and obtained a substantially lower $Co^{II/III}$Cyt *c* self-exchange rate constant of 1.6×10^{-4} M^{-1} s^{-1}; however, our calculations with the same inputs ($-\Delta G^{\circ} = 0.40$ eV, k_{22} = 8100 M^{-1} s^{-1}, collision frequency *Z* assumed to be $\sim 1 \times 10^{11}$ M^{-1} s^{-1}, work term $W_{12} \approx 1$ since charges and radii are the same for the self- and cross-reactions) give a value of 5.3×10^{-3} M^{-1} s^{-1} and $f_{12} = 0.27$.

It is also possible to estimate the $Co^{II/III}$Cyt *c* self-exchange rate constant from our rate measurements on the oxidation of cobaltocytochrome *c* by hexaammineruthenium(III) using the Marcus cross-relation. Due to the widely different sizes and charges of the reactants, the work term W_{12} needs to be explicitly considered; we will use the value of 1.9 calculated by Marcus and Sutin for the reaction of $[Ru^{II}(NH_3)_6]^{2+}$ and Fe^{III}Cyt *c* (ref 27, Table VII).[32] We have measured the reduction potential of $[Ru^{II}(NH_3)_6]^{3+}$ in 50 mM pH 7 sodium phosphate buffer as −0.008 V vs NHE;[33] the driving force for reaction 7 is therefore 0.13 eV. Taking our observed rate constant of 10 M^{-1} s^{-1} and the reported self-exchange rate constant of hexaammineruthenium(III/II), 3200 M^{-1} s^{-1},[34] we obtain an estimated $Co^{II/III}$Cyt *c* self-exchange rate constant of 5.7×10^{-5} M^{-1} s^{-1} ($f_{12} = 0.88$). This value is a factor of 100 lower than that calculated from the protein cross-reaction; however, such variation is not unusual in comparisons of this type.

Both results provide quantitative estimates of the slowness of self-exchange in CoCyt *c* which place it among complexes such as $Co(en)_3^{2+/3+}$ (2.0×10^{-5} M^{-1} s^{-1}),[35] $Co(Me_4[14]\text{-tetraeneN}_4)(H_2O)_2^{2+/3+}$ (5.0×10^{-2} M^{-1} s^{-1}),[36] $Co(Me_6[14]4,11\text{-dieneN}_4)(H_2O)_2^{2+/3+}$ (4.5×10^{-5} M^{-1} s^{-1}),[36] $Co([14]\text{aneN}_4)(H_2O)_2^{2+/3+}$ (8.0×10^{-4} M^{-1} s^{-1}),[36] and $Co([15]\text{aneN}_4)(H_2O)_2^{2+/3+}$ (6.0×10^{-3} M^{-1} s^{-1}),[36] as opposed to

(28) Seki, H.; Imamura, M. *Biochim. Biophys. Acta* **1981**, *635*, 81−89.
(29) Hopfield, J. J. *Proc. Natl. Acad. Sci. U.S.A.* **1974**, *71*, 3640−3644.
(30) Marcus, R. A.; Sutin, N. *Inorg. Chem.* **1975**, *14*, 213−216.
(31) Marcus, R. A.; Sutin, N. *Biochim. Biophys. Acta* **1985**, *811*, 265−322.
(32) Reference 31, Table VII. There is also a work term correction to f_{12} (see ref 31, eqs 23−25) which is ∼4%, small enough to be neglected in this treatment.
(33) Su, C.; Wishart, J. F. Unpublished results.
(34) Brown, G. M.; Sutin, N. *J. Am. Chem. Soc.* **1979**, *101*, 883−892.
(35) Przystas, T. J.; Sutin, N. *J. Am. Chem. Soc.* **1973**, *95*, 5545.
(36) Endicott, J. F.; Durham, B.; Kumar, K. *Inorg. Chem.* **1982**, *21*, 2437−2444.

complexes like $Co(phen)_3^{3+}$ (45 M^{-1} s^{-1})[37] and $Co(sep)^{3+}$ (5.1 M^{-1} s^{-1}),[38] where metal−ligand bond length changes are smaller. The effects of nonadiabaticity in the protein case must be remembered; however, the slow self-exchange rate implies that there are significant axial bond length changes between the oxidation states of CoCyt *c*. Since CoCyt *c* is low spin in both oxidation states,[9,21] it is the σ-antibonding, axial d_{z^2} orbital which is populated when Co^{III}Cyt *c* is reduced. Moore et al.[10] have deduced from NMR measurements that the $Co-S(Met_{80})$ bond length in Co^{III}Cyt *c* is shorter than the $Fe-S(Met_{80})$ bond length in Fe^{II}Cyt *c*. It is reasonable to expect that the $Co^{II}-S(Met_{80})$ bond is appreciably longer.

An estimate of the increase in reorganization energy when cobalt is substituted for iron in horse-heart cytochrome *c* can be made from examination of the relative self-exchange rates. The standard model[31] for outer-sphere electron transfer describes a three-step process: outer-sphere precursor formation (K_{OS}), rate-determining electron transfer (k_{ET}), and successor dissociation:

$$\text{MCyt } c^{III} + {}^*\text{MCyt } c^{II} \overset{K_{OS}}{\rightleftharpoons} \{\text{MCyt } c^{III}\cdot{}^*\text{MCyt } c^{II}\} \quad (12)$$

$$\{\text{MCyt } c^{III}\cdot{}^*\text{MCyt } c^{II}\} \overset{k_{ET}}{\rightleftharpoons} \text{MCyt } c^{II}\cdot{}^*\text{MCyt } c^{III} \quad (13)$$

$$\{\text{MCyt } c^{II}\cdot{}^*\text{MCyt } c^{III}\} \rightleftharpoons \text{MCyt } c^{II} + {}^*\text{MCyt } c^{III} \quad (14)$$

This mechanism is related to the overall self-exchange reaction by $k_{obs} = K_{OS}k_{ET}$. Because the protein charges and dimensions are essentially the same whether they contain iron or cobalt, the precursor formation constant K_{OS} should be the same for the two cases. The electron transfer rate k_{ET} within the precursor complex depends on the electronic transmission coefficient κ_{el}, the nuclear frequency factor ν_n, and the free energy barrier of reorganization ΔG^*_r:

$$k_{ET} = \kappa_{el}\nu_n\, e^{-\Delta G^*_r/RT} \quad (15)$$

We will assume that κ_{el} and ν_n do not vary between the iron and cobalt cases; thus all the difference in self-exchange rates is ascribed to the reorganization barrier.[45] In the general case, the reorganization barrier is given by

$$\Delta G^*_r = (\lambda_{12}/4)\left(1 + \frac{\Delta G^\circ_{12} + w_{21} - w_{12}}{\lambda_{12}}\right)^2 \quad (16)$$

$$\lambda_{12} = (\lambda_{11} + \lambda_{22})/2 \quad (17)$$

In the case of self-exchange, eq 16 simplifies to $\Delta G^*_r = (\lambda_{11}/4)$. Depending on the ionic strength and other factors, the self-exchange rate of FeCyt *c* ranges between 300 and 8000 M^{-1} s^{-1} at 25 °C.[25,39] Taking the calculated value of 350 M^{-1} s^{-1} for $\mu = 0.1$ M and 25 °C, and using the geometric mean of the estimated self-exchange rates for cobalt (5.5×10^{-4} M^{-1} s^{-1}), we obtain a rate ratio $k_{Fe}/k_{Co} \approx 6.5 \times 10^5$.

$$\frac{k_{Fe}}{k_{Co}} = \frac{e^{-\lambda_{Fe}/4RT}}{e^{-\lambda_{Co}/4RT}} \quad (18)$$

From eq 18 we obtain $\lambda_{Co} - \lambda_{Fe} = 1.4$ eV. Using $\lambda_{Fe} = 1.0$ eV,[7,31] $\lambda_{Co} = 2.4$ eV. The rather large reorganization energy calculated here is consistent with Chien's estimate of 2.0 eV obtained from the application of nonadiabatic multiphonon electron-tunneling theory to several cross-reactions of CoCyt *c*.[21,45]

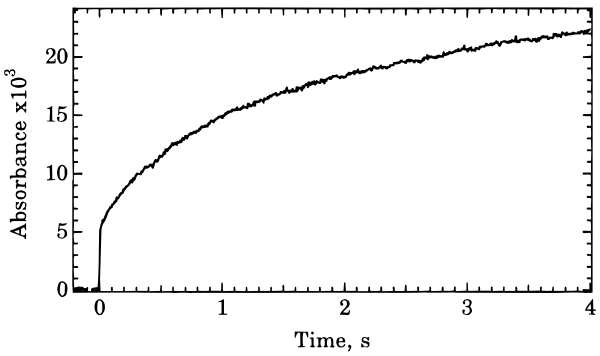

Figure 7. Typical 434 nm pulse radiolysis transient absorption plot for intramolecular electron transfer in $(NH_3)_5Ru^{III}(His_{33})$ horse-heart cobaltocytochrome *c* at 25 °C.

(e) Intramolecular Electron Transfer in $(NH_3)_5Ru^{III}-Co^{II}$Cyt *c*. The rate of intramolecular electron transfer from Co^{II} to Ru^{III} in $(NH_3)_5Ru^{III}-Co^{II}$Cyt *c* was measured by pulse radiolysis using the following reaction scheme:

$$(NH_3)_5Ru^{II}-Co^{II}\text{Cyt } c + N_3^\bullet \rightarrow (NH_3)_5Ru^{II}-Co^{III}\text{Cyt } c + N_3^- \quad (19)$$

$$(NH_3)_5Ru^{II}-Co^{II}\text{Cyt } c + N_3^\bullet \rightarrow (NH_3)_5Ru^{III}-Co^{II}\text{Cyt } c + N_3^- \quad (20)$$

$$(NH_3)_5Ru^{III}-Co^{II}\text{Cyt } c \rightarrow (NH_3)_5Ru^{II}-Co^{III}\text{Cyt } c \quad (21)$$

Reaction 19 leads directly to the final product through the direct oxidation of cobaltocytochrome *c* by the azide radical with a rate constant of about 8×10^8 M^{-1} s^{-1}. The rate of oxidation of the protein-bound $(NH_3)_5Ru^{II}-$ group by the azide radical (reaction 20) to generate the desired electron transfer precursor should be similar to the value of 2×10^9 M^{-1} s^{-1} estimated for the iron case. Due to the fact that the rate constant for reaction 20 is over twice as large as that for reaction 19, most of the azide radical formed by pulse radiolysis reacts to form the $Ru^{III}-Co^{II}$ intermediate which undergoes intramolecular electron transfer by reaction 21. The progress of reaction 21 is easily followed at 434 nm, where the absorbance increase due to the Soret shift to longer wavelengths upon oxidation is largest. A typical transient-absorption trace is shown in Figure 7. Due to the fact that it is difficult to keep all of the cobaltocytochrome reduced during the experiment, some of the Ru^{III} centers will be created on cytochrome which is already oxidized; reduction of these centers must proceed by an intermolecular process, which accounts for the rise in absorbance at longer times. Consequently, a biexponential fit was used. As a given sample was repeatedly pulsed, the effect of the accumulated dose was to decrease the absorbance change associated with the first, intramolecular electron transfer process, while the observed rate remained the same. The later process, however, slowed down with each subsequent pulse, indicating that it was probably intermolecular in nature.

Given the experimental difficulties of doing kinetic experiments with the reduced form of CoCyt *c*, it is reasonable for the reader to wonder why a reductive method was not used, such as using $CO_2^{\bullet-}$ to reduce the $Ru^{III}-Co^{III}$ form to generate the $Ru^{III}-Co^{II}$ intermediate. The primary reason is the slow self-exchange rate of CoCyt *c* compared to that for the

(37) Sailasuta, N.; Anson, F. C.; Gray, H. B. *J. Am. Chem. Soc.* **1979**, *101*, 455−458.
(38) Creaser, I. I.; Geue, R. J.; Harrowfield, J. MacB.; Herlt, A. J.; Sargeson, A. M.; Snow, M. R.; Springborg, J. *J. Am. Chem. Soc.* **1982**, *104*, 6016−6025.
(39) Gupta, R. K. *Biochim. Biophys. Acta* **1973**, *292*, 291−295.

ruthenium complex. Most of the reducing radicals would react directly with the ruthenium group, resulting in the production of very small fractions of the $Ru^{III}-Co^{II}$ intermediate. For example, in the case of $CO_2^{\bullet-}$, the rates are 5×10^9 and 1.4×10^8 M^{-1} s^{-1}, respectively, for reduction of the ruthenium[3] and cobalt centers. The 2-propanol radical ($(CH_3)_2C^{\bullet}OH$) was also tried, since Isied and co-workers[3] found that it had a higher tendency to directly reduce the heme in $(NH_3)_5Ru^{III}-Fe^{III}$Cyt *c*. However, in the case of $(NH_3)_5Ru^{III}-Co^{III}$Cyt *c*, there was no significant improvement in the fraction of Co^{III} reduction for the 2-propanol radical over $CO_2^{-\bullet}$.

The intramolecular electron transfer rate constant for reaction 21 is 1.28 ± 0.04 s^{-1} at 25 °C for a driving force of 0.28 ± 0.02 eV. The same rate was measured at $(NH_3)_5Ru^{II}-Co^{II}$Cyt *c* concentrations of 1.7, 3.25, 4.0, and 11.8 μM, removing the possibility that the observed rate is due to a bimolecular process. The rate constant for intramolecular Ru^{II}-to-Fe^{III} electron transfer in horse-heart $(NH_3)_5Ru^{II}(His_{33})-Fe^{III}$Cyt *c* was reported to be 53 ± 2 s^{-1} at 25 °C ($\Delta H^{\ddagger} = 3.5 \pm 0.2$ kcal/mol, $\Delta S^{\ddagger} = -39 \pm 1$ cal/(deg mol)) by Isied and co-workers[3] under conditions similar to ours. Although this electron transfer process occurs in the opposite direction than in the cobalt-substituted cytochrome *c* case, we can use the previously reported Ru^{II}-to-Fe^{III} electron transfer rate and eqs 15−18 to calculate a predicted rate in the cobalt case. Taking $\lambda_{Fe} = 1.0$ eV,[7,31] $\lambda_{Co} = 2.4$ eV from above, and $\lambda_{Ru} = 1.2$ eV,[7,31,34] we obtain $\lambda_{FeRu} = 1.1$ eV and $\lambda_{CoRu} = 1.8$ eV. The driving force for Ru^{II}-to-Fe^{III} electron transfer is 0.125 eV. The work terms w_{21} and w_{12} in eq 16 do not apply in the intramolecular case. We again assume that the electronic transmission coefficient κ_{el} and the nuclear frequency factor ν_n do not vary between the iron and cobalt systems. From eq 16 we obtain $\Delta G^*_{r,FeRu} = 0.216$ eV and $\Delta G^*_{r,CoRu} = 0.321$ eV. The resulting estimated intramolecular Co^{II}-to-Ru^{III} electron transfer rate constant from eq 18 is 0.9 s^{-1}, close to the observed rate. This agreement validates the assumption that κ_{el} (or more precisely, the product $\kappa_{el}\nu_n = 2.4 \times 10^5$ s^{-1}) is the same for the intramolecular electron transfer process in both the ruthenium ammine-modified iron and cobalt proteins, and therefore, if discrete electron transfer pathways[40,41] operate in this system, they are not destroyed by the process of replacing iron with cobalt.

The rate of intramolecular electron transfer in $(NH_3)_5Ru^{III}-Co^{II}$Cyt *c* was also measured at temperatures ranging from 6.8 to 35.3 °C (see Table S1 of the Supporting Information). The Eyring plot shown in Figure 8 yielded the following activation parameters: $\Delta H^{\ddagger} = 5.7 \pm 0.2$ kcal mol^{-1}, $\Delta S^{\ddagger} = -38.7 \pm 0.5$ cal deg^{-1} mol^{-1}. The rate and activation parameters for uphill Fe^{II}-to-Ru^{III} electron transfer in horse-heart $(NH_3)_5Ru(His_{33})$-FeCyt *c* were recently determined to be $k = 0.40 \pm 0.01$ s^{-1}, $\Delta H^{\ddagger} = 12.5 \pm 0.2$ kcal mol^{-1}, and $\Delta S^{\ddagger} = -18.3 \pm 0.7$ cal deg^{-1} mol^{-1}, in 50 mM pH 7.0 phosphate buffer.[42] Although the rates for the cobalt and iron systems at 25 °C are very similar, comparison of the activation parameters indicates some major differences. The smaller activation enthalpy in the cobalt case points toward a greater exothermicity for the cobalt oxidation process, perhaps due to a preference of the protoporphyrin IX ring for the smaller Co^{III} cation over the larger Co^{II} ion. Counteracting the favorable enthalpy change when the cobalt center is oxidized is a large decrease in entropy, which shows up as a 20 cal deg^{-1} mol^{-1} decrease in the activation entropy of the cobalt system compared to the iron system. This effect may indicate significant loss of vibrational and conformational degrees of freedom in the protein as a result of the tighter axial ligation in the Co^{III} form. Another contribution to the entropy may come from an increase in the number of tightly bound water molecules. The larger entropy loss upon oxidation in the cobalt case can also be seen when the activation entropy for the oxidation of Co^{II}Cyt *c* by Fe^{III}Cyt *c* (−33 cal deg^{-1} mol^{-1})[21] is compared with that for $Fe^{II/III}$Cyt *c* self-exchange (−17 cal deg^{-1} mol^{-1}).[39] These conjectures await further examination of the redox thermodynamics of CoCyt *c*, which is ongoing in our laboratory.

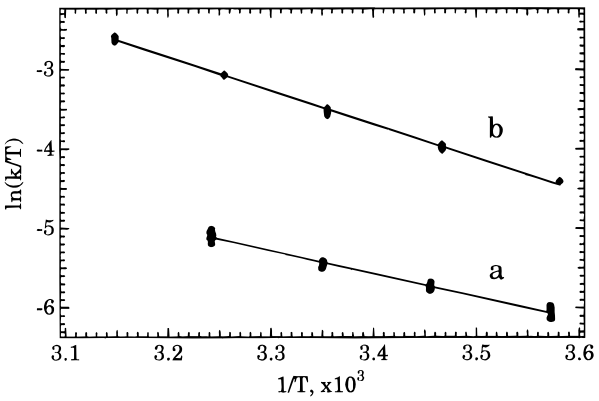

Figure 8. Eyring plots of the observed rate of intramolecular electron transfer in pentaammineruthenium-modified horse-heart cobaltocytochrome *c* (a) and the observed rate of intermolecular oxidation of cobaltocytochrome *c* by $[Ru(NH_3)_6]^{3+}$ (b).

The present results can also be compared with measurements of electron transfer rates in pentaammineruthenium-modified, zinc-substituted horse heart cytochrome *c* by Elias et al.,[6a] as further interpreted by Meade et al.[6b] In these experiments, both reductive and oxidative electron transfer quenching of the Zn-porphyrin (ZnP*) triplet excited state was observed by transient absorption techniques ($k_{Ru^{II}\rightarrow ZnP^*} = 2.4 \times 10^2$ s^{-1}, $\Delta G^{\circ} = -0.30$ eV[44] ; $k_{ZnP^*\rightarrow Ru^{III}} = 7.7 \times 10^5$ s^{-1}, $\Delta G^{\circ} = -0.76$ eV[44]). In addition, the rate of back electron transfer after oxidative quenching was also measured ($k_{Ru^{II}\rightarrow ZnP^{\bullet+}} = 1.6 \times 10^6$ s^{-1}, $\Delta G^{\circ} = -0.95$ eV[44]). The reductive quenching process involves electron transfer from ruthenium(II) into a relatively low-lying orbital of the ZnP* moiety; as such, the reaction energetics are similar to those of the ground-state electron transfer systems involving FeCyt *c* and CoCyt *c*. Taking $\lambda = 1.2$ eV,[6b] one obtains $\Delta G^*_{r,ZnRu} = 0.169$ eV. On the basis of observed rate in the Ru^{II}-to-Fe^{III} system, for the Ru^{II}-to-ZnP* process $k_{calc} =$

(40) Regan, J. J.; Risser, S. M.; Beratan, D. N.; Onuchic, J. N. *J. Phys. Chem.* **1993**, *97*, 13083−13088.
(41) Siddarth, P.; Marcus, R. A. *J. Phys. Chem.* **1993**, *97*, 13078−13082.
(42) Sun, J.; Isied, S. S.; Wishart, J. F. *Inorg. Chem.* **1995**, *34*, 3998−4000.
(43) Cohen, D. S.; Pielak, G. J. *J. Am. Chem. Soc.* **1995**, *117*, 1675−1677.

(44) The following half-cell potentials vs NHE from ref 6b were used to calculate the driving forces: $ZnP^{\bullet+/0}$, 1.09 V; $ZnP^{\bullet+/*}$, −0.62 V; $ZnP^{*/\bullet-}$, 0.44 V. Instead of using the potential of the model complex $(NH_3)_5Ru^{III/II}$(His) (0.08 V) as in ref 6b, we shall use the observed potential of the $(NH_3)_5Ru^{III/II}(His_{33})$ complexes of FeCyt *c* and CoCyt *c*, 0.14(1) V vs NHE. Attempts to measure the redox potential of $(NH_3)_5Ru^{III/II}(His_{33})-$ZnCyt *c* by differential pulse voltammetry at a dipyridyl disulfide-treated gold electrode were unsuccessful.[33]
(45) (a) Theoretical calculations on the $[Fe(H_2O)_6]^{2+/3+}$ and $[Co(NH_3)_6]^{2+/3+}$ self-exchange reactions by Newton[45b] suggest that electronic coupling is stronger for low-spin cobalt than for low-spin iron, due to orbital occupancy/symmetry and radial extent differences. It is difficult to be quantitative about transferring the above results to a *c*-type heme environment. One difference is that the heme, histidine, and methionine ligands have π-interactions with the central metal, which may reduce the difference between iron and cobalt. If, however, coupling is stronger in the cobalt case, then the estimated reorganization energy of 2.4 eV for CoCyt *c* might be a *lower* limit. This coupling question affects the inter- and intramolecular redox reactions in the same way, so subsequent inferences (*vide infra*) about the integrity of the intramolecular ET "pathway" upon metal substitution are not affected. (b) Newton, M. D. *J. Phys. Chem.* **1988**, *92*, 3049−3056.

340 s^{-1}, not far from the observed value of 240 s^{-1}. (It must be remembered, however, that the electron acceptor in this case is the porphyrin ring and not the metal center; therefore, the coupling between the redox centers is likely to be different from that in the FeCyt *c* and CoCyt *c* cases.) In the cases of oxidative excited state quenching and back electron transfer, the porphyrin redox states are highly reducing (−0.62 V vs NHE) and highly oxidizing (1.09 V vs NHE), respectively. Coupling between the two redox centers is enhanced in these two cases due to the energetic proximity of intervening states of the protein matrix bridging the two centers, resulting in values of $\kappa_{el}\nu_n = (3-4) \times 10^6$ s^{-1}, over a factor of 10 greater than that for the reactions in the low-energy regime.

Conclusion

Substitution of cobalt for iron in horse-heart cytochrome *c* has previously been shown by NMR[10] and other physical studies[9] to result in conservation of a native-like structure. Cobalticytochrome *c* is resistant to enzymatic proteolysis, which is consistent with the substitution inertia of Co^{III}. Modification of CoCyt *c* with the pentaammineruthenium moiety proceeds with the same efficiency as with the native form. Intramolecular Co^{II}-to-Ru^{III} electron transfer is slow, 1.28 s^{-1}, despite a 0.4 eV increase in driving force, due to a large reorganization barrier contribution from the cobalt center. The electronic transmission coefficients between the two metal sites appear to be nearly the same in the iron and cobalt cases. The results suggest that the process of cobalt substitution does not disrupt the electronic coupling mechanism, in whatever form it takes. It is also significant in that it opens the way for a new series of derivatives with the same degree of electronic coupling between centers. In further studies, we will examine the effect of increasing the driving force further using higher-potential ruthenium complexes and we will measure rates of intramolecular electron transfer in other substituted cytochromes with substantially lower reorganization barriers.

Acknowledgment. This research was carried out at Brookhaven National Laboratory under Contract DE-AC02-76CH00016 with the U.S. Department of Energy and supported by its Division of Chemical Sciences, Office of Basic Energy Sciences. The authors wish to thank Prof. Stephan S. Isied, Dr. Rolf Bechtold, and Prof. I-Jy Chang for helpful advice.

Supporting Information Available: HPLC chromatograms measured at 300 nm and 420 nm corresponding to the 220 nm data shown in Figures 4 and 5, circular dichroism spectra of horse-heart cobaltocytochrome *c*, ferrocytochrome *c*, and ferricytochrome *c*, a differential pulse voltammogram of $(NH_3)_5Ru-$CoCyt *c*, a plot of intermolecular electron transfer rates as a function of $[(NH_3)_6Ru]^{3+}$ concentration, and a table of observed rates of intermolecular and intramolecular electron transfer as functions of temperature (12 pages). Ordering information is given on any current masthead page.

IC960715W